NUMERICAL COMPUTATION OF THE THERMAL SELF-ACTION EFFECT IN A SUBSONIC GAS FLOW

A. N. Kucherov and E. V. Ustinov

UDC 534.211+533.6

Results are obtained on the thermal self-action effect of an initially Gaussian beam in a subsonic weakly-absorbent gas flow in a broad range of similarity parameters.

The thermal self-action effect [1-3] in a homogeneous gas flow [4, 5] has been investigated well up to now for convective [6] and supersonic [7] gasdynamic modes. Individual computations have been performed for the heat conductive [8] and subsonic [9-11] modes. Finite difference schemes (explicit [12] and implicit [13]), the finite elements method [14], and the method of discrete Fourier transform using the fast Fourier transform [10, 15, 16] have been used to construct the solution of the paraxial optics equation. A distinct degree of efficiency was detected for some algorithms in different self-action modes and conditions. For instance, application of the method of expansion in discrete Fourier series yields more accurate results (other conditions being equal) for moderate Fresnel numbers comparable to one, while the explicit finite-difference scheme is better for high numbers. This latter scheme was applied successfully to investigate the supersonic mode, but it is less convenient and suitable for the other modes. The algorithm of [12] yields less accurate results for high values of the self-action parameter (than the implicit scheme). The Krank–Nicholson implicit scheme yields less accurate results for large Fresnel numbers than does the implicit scheme. The algorithms for construction of the solution manifest a considerable sensitivity to a change in the number M. This is because the type of the gasdynamics equations changes during passage from one mode to another. The present paper is devoted to a study of the thermal self-action effect in the subsonic mode for which the flow velocity is the same order as the speed of sound in an unperturbed medium. In the papers mentioned above devoted to the subsonic mode, the results are sparse and incomplete, so that it is impossible to set up a complete set of similarity parameters and it is impossible to make a quantitative comparison. In this connection, comparison of the results obtained by using different algorithms in this paper is quite important.

The propagation process for a beam with small divergence in a moving weakly absorbent medium is described by the following system of dimensionless equations and boundary conditions

$$2F\frac{\partial u}{\partial z}+i\nabla_{\perp}^{2}u=-[2iFN\rho_{1}(I,\ M)+FN_{\alpha}]\,u, \tag{1}$$

$$u|_{z=0}=u_{0}(x,\ y);\ u|_{x,\,y\to\pm\infty}\to 0, \tag{2}$$

$$\left[(1-M^{2})\frac{\partial^{2}}{\partial x^{2}}+\frac{\partial^{2}}{\partial y^{2}}\right]\frac{\partial\rho_{1}}{\partial x}=-\nabla_{\perp}^{2}I(x,\ y,\ z), \tag{3}$$

$$\rho_{1}|_{x\to-\infty}\to 0,\ \left.\frac{\partial\rho_{1}}{\partial x}\right|_{x,\,y\to\pm\infty}\to 0. \tag{4}$$

Here $I = uu^{*}$ is the radiation intensity and $\Delta\rho/\rho_{0} = \varepsilon\rho_{1}$. The x,y coordinates transverse to the beam are referred to the radius a, the longitudinal coordinate z is referred to the characteristic track length L, and the field function to $\sqrt{I_{0}}$. We select the initial distribution Gaussian $u_{0} = \exp\{-(x^{2} + y^{2})/2\}$.

A dimensionless formulation of the problem is convenient in that it permits diminishing the number of parameters being given by more than twice. The dimensionless parameters characterize the role and influence of various physical factors: diffraction, molecular absorption, thermal self-action, acoustics, and forced convection. It is natural to take the

Translated from Inzhenerno-Fizicheskii Zhurnal, Vol. 8, No. 1, pp. 35-42, January, 1990. Original article submitted May 31, 1988.

0022-0841/90/5801-0028$12.50

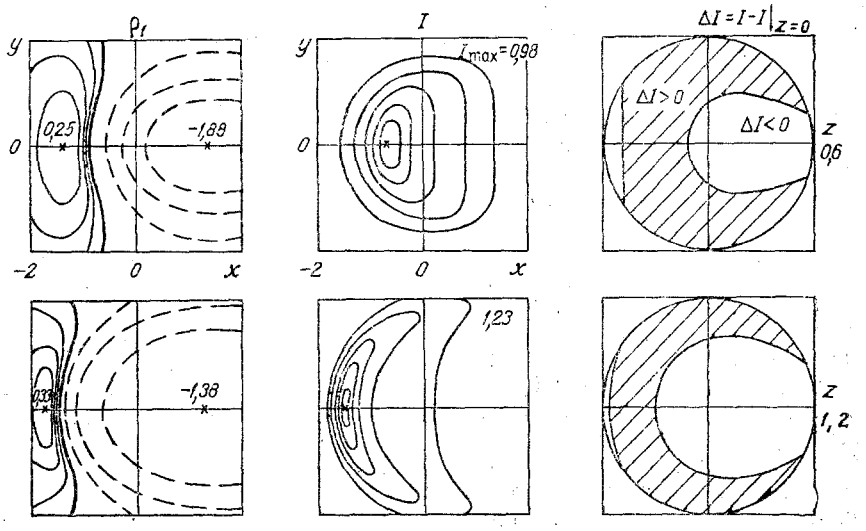

Fig. 1. Isochores, isophots, domains of amplification (shaded) and diminution of the intensity in comparison with the initial section M = 0.8, F = 5, N = 1, N_α = 0.

thermal self-action length as the characteristic extent of the track for a study of the thermal self-action effect. We shall henceforth consider the self-action parameter to equal one: N = 1.

The manifold of numerical schemes and methods of solving the problem under consideration is due, as already noted, to the suitability and efficiency of the algorithm in application to a specific problem being solved, to a specific mode, to specific conditions that similarity parameters can characterize. As a rule, the order of the approximation is indicated for the algortihms listed in the introduction, but there is no strict proof of the stability and convergence. The authors are interested primarily in the practical realization and results.

A strict mathematical foundation is given for the algorithm in [16] under the assumption that the right side of (1) is a known function of u. The crux of the algorithm is the following. We expand the field function u, the right side of (1), and the initial distribution $u_0(x, y)$ in a discrete Fourier series in a sufficiently large domain $[L_x, L_y]$ with sufficiently shallow steps Δx, Δy. We consequently obtain a nonlinear ordinary differential equation (the coordinate z is the independent variable) for the spectrum coefficients of the function u. Linearizing by a simple iteration process and solving this equation by some method, we find the spectral coefficients and therefore the desired field function. The relation between the functions ρ_1 and u that is given by (3) can be determined by expansions in either discrete complex exponential [10] or sine and cosine Fourier series (details will be mentioned below).

The algoirthm described was realized for computations on an electronic computer in several modifications of the organization of the iteration process. The quantity of iterations for a given computation error not higher than one percent turned out to be within reasonable limits (5-6) just for small values of the Fresnel number (of the order of one) and for $F \gtrsim 5$ the quantity of the iterations grows to 10-15. The machine time of the computation increases substantially. Application of the Newton method or gradient methods (steepest descent method, say) causes growth of the expenditure in the machine memory and consequently does not yield the desired machine time reduction. These circumstances produce inconvenience for massive parametric computations.

As is shown in [10], the second order of the approximation has the following scheme:

$$u^{j+1} = \exp\left\{-\left(\frac{i}{2F}\nabla_\perp^2 + \frac{N_\alpha}{2}\right)\frac{\Delta z}{2}\right\} \exp\left\{-iFN\int_{z_j}^{z_j+\Delta z}\rho_1(z')\,dz'\right\} \times$$
$$\times \exp\left\{-\left(\frac{i}{2F}\nabla_\perp^2 + \frac{N_\alpha}{2}\right)\frac{\Delta z}{2}\right\} u^j. \qquad (5)$$

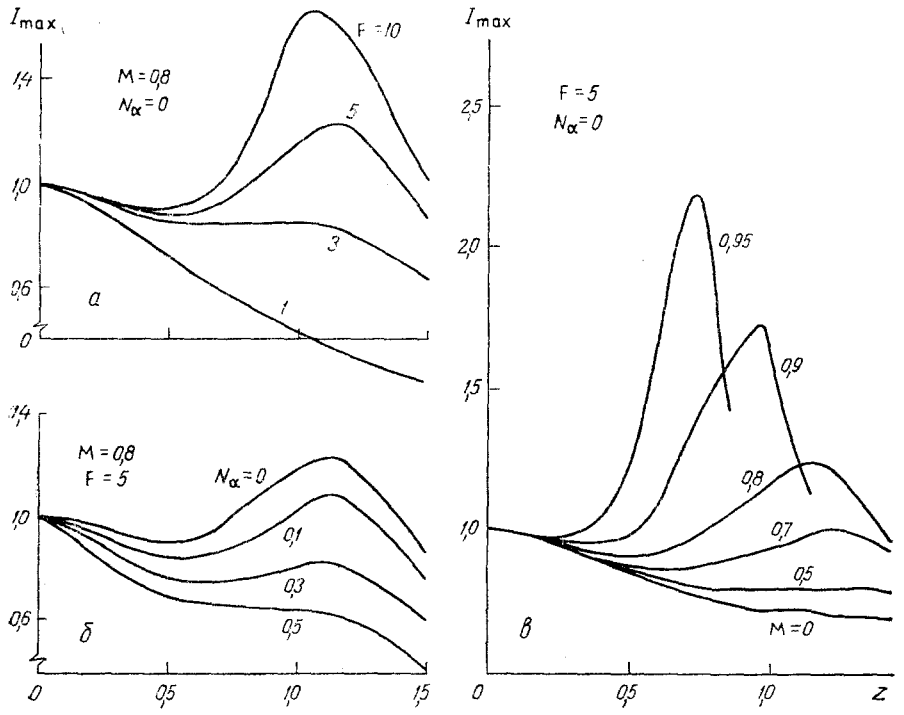

Fig. 2. Dependences of the maximal intensity $I_{max}(z)$ for a Gaussian beam in the subsonic mode of thermal self-action for similarity parameter variations: a) F; b) N_α; c) M.

The field function is expanded in Fourier series for whose summation the fast Fourier series for whose summation the fast Fourier transform is usually utilized. Conversion from the j-th layer in z to the (j + 1)-th includes three sequential steps. At the beginning we calculate the diffraction perturbation and the moleculear attentuation of the beam at a half-step $\Delta z/2$ distance (the action of the nearest operator on the function u^j). We use the field function obtained to determine the main terms of the density perturbation ρ_1 according to (3) and we compute the self-action in the step Δz (the action of the mean operator on the field function obtained in the first step). In the third, concluding, step, we calculate the diffraction perturbation and molecular attenuation in the second half-step $\Delta z/2$ (the action of the third operator of (5) on the field function obtained earlier). Later the third and first steps can be combined in order to reduce machine computation time. However, before printing the results (graphs), the next diffraction half-step must be made to calculate the desired field function at a node standing an integer number of steps Δz off from the initial section. For intermediate nodes standing off $\Delta z/2$ from those mentioned above, the scheme (5) does not yield a second order of appoximation.

The main part of the results of this paper is obtained by using the algorithm described. A simplified modification is proposed in [15], that includes two steps: calculation of the diffraction perturbations at the step Δz at the beginning and then calculation of the perturbed density and computation of the self-action. This algorithm is simpler in realization but is of first order of approximation in the coordinate x. Comparative computations using all the algorithms described above are executed for certain modifications. Good correspondence is obtained within the limits of the error in the approximation.

Let us turn to an elucidation of the results. The computed domain was selected such that L_x = 6.4, 12.8; L_y = 6.4, 12.8, 25.6. The number of nodes of the computational mesh was N_x = 64, 128 and N_y = 64, 128, and the maximal step of the computational mesh is Δx = 0.1; Δy = 0.1. The fundamental volume of calculations is executed for L_x = 6.4; L_y = 6.4; Δx = 0.1; Δy = 0.1; Δz = 0.1; N_x = 64; N_y = 64.

Changes in the initially collimated Gaussian beam along the track in the subsonic flow (M = 0.8) are shown in Fig. 1. The attenuation parameter was assumed zero (N_α = 0). The Fresnel number is sufficiently large (F = 5) so that the diffraction deliquescence does not predominate over the focusing due to the thermal self-action. Equal density contours are represented (on the left: $0.75\rho_{1max}$, $0.5\rho_{1max}$, $0.25\rho_{1max}$; ρ_1 = 0, $0.75\rho_{1min}$, $0.5\rho_{1min}$,

$0.25\rho_{1\min}$), as are equal intensity contours (at the middle: $0.9I_{\max}$, $0.75I_{\max}$, $0.5I_{\max}$, $0.25I_{\max}$, $0.1I_{\max}$) and domains of intensity amplification ($\Delta I = I - I|_{z=0} > 0$, shaded) and diminution ($\Delta I < 0$, unshaded). contours with negative values of the density function ρ_1 are superposed by dashed lines, the contour $\rho_1 = 0$ is extracted by a heavy curve. The beam is broadened to approximately the distance $z_{\text{phys}} = 0.6z_T$ and the intensity peak diminishes. Intensity peak shifting simultaneously occurs upstream in the gas in the density growth domain. The perturbed gas in this domain acts as a collecting lens on the radiation. The intensity peak (its location is indicated by the cross) starts to grow and the beam is focused as a whole in the section $z = 1.2$ as a comparison of the intensity amplification and diminution domains shows. The effective transverse beam dimension diminished during focusing and the defocusing influence of the diffraction gradually grows. Consequently, the magnification of the beam intensity is continued just to a certain section that can provisionally be called focal. In the example under consideration it is located at $z_{\text{phys}} \approx 1.15z_T$. Beyond this section the intensity peak decreases rapidly. The isochore pattern does not undergo qualitative changes along the beam path, there are a rarefaction domain in the thermal wake and a gas compression domain in the windward part of the beam. In place of the concentric circles the isophots acquire a crescent shape.

Changes in the intensity peak along the track are represented in Fig. 2 for changes in the similarity parameters: a) the Fresnel number $F = 1$-10 ($M = 0.8$; $N_\alpha = 0$); b) the absorption parameters $N_\alpha = 0.5$ ($M = 0.8$; $F = 5$); c) the Mach number $M = 0$-0.95 ($F = 5$, $N_\alpha = 0$). The convective mode ($M = 0$) is included for completeness of the investigation as the limit case as $M \to 0$. Modifications cause special interest in nonlinear optics when the beam is propagated a significant distance for a negligible change in the intensity peak (or a certain neighborhood of it), the so-called quasi-waveguide modes [1-3, 6, 17]. The results presented above show that in contrast to the supersonic modes sufficiently protracted quasi-waveguide sections of the track are not observed in the subsonic mode. The length of such sections is an order of magnitude less than the thermal self-action length.

As the number M approaches one the perturbation domain of the gasdynamic quantities grows, as is known, especially in the direction transverse to the velocity vector. Denstiy and intensity perturbations are increased radically, and the length of thermal self-action is shortened [5]. As in [8], it is convenient to extract the "isobaric" and acoustic components of the density perturbations

$$\rho_1 = \rho_{1,1} + \rho_{1,2};\ \rho_{1,1} = -\int_{-\infty}^{x} I(x',\ y,\ z)\,dx' \tag{6}$$

for investigation of the near-sound domain of Mach numbers (but not yet transonic $|M - 1| > \varepsilon^{2/3}$). Then the "acoustic" component (that is proportional to the pressure perturbation) satisfies the Poisson equation

$$(1 - M^2)\frac{\partial^2 \rho_{1,2}}{\partial x^2} + \frac{\partial^2 \rho_{1,2}}{\partial y^2} = -M^2 \frac{\partial I}{\partial x}, \tag{7}$$

$$\rho_{1,2}|_{x,\,y \to \pm\infty} \to 0. \tag{8}$$

The method of expansion in discrete Fourier series is used to construct the solution of this equation as for (3), however, the expansions are in the sines and cosines (and not in the complex exponentials):

$$\rho_{1,2} = \sum_m \sum_n \rho_{mn} \sin\left[\frac{\pi m (x + L_x/2)}{L_x}\right] \sin\left[\frac{\pi n (y + L_y/2}{L_y}\right], \tag{9}$$

$$I = \sum_m \sum_n I_{mn} \cos\left[\frac{\pi m (x + L_x/2)}{L_x}\right] \sin\left[\frac{\pi n (y + L_y/2)}{L_y}\right]. \tag{10}$$

The expression (9) permits automatic satisfaction of the boundary conditions on the mesh domain boundary for $x = \pm L_x/2$, $y = \pm L_y/2$. The equation (7) yields the following algebraic relation between the spectral coefficients

$$\rho_{mn} = -I_{mn} \frac{\pi m M^2/L_x}{(1 - M^2)(\pi m/L_x)^2 + (\pi n/L_y)^2}. \tag{11}$$

The algorithm (6)-(11) and the above-mentioned algorithm to calculate the density perturbation by using expansions in complex exponentials [10] were realized in parallel and dis-

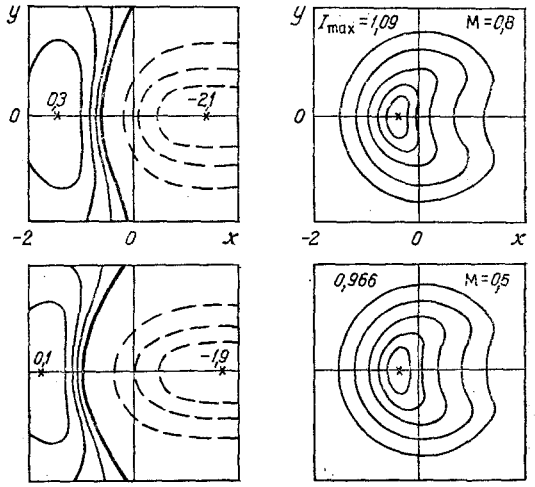

Fig. 3. Isochores and isophots in the near field of a Gaussian beam in subsonic flow of a weakly absorbing gas obtained by using the linearized solution. M = 0.6 and 0.8, $F \gg 1$; $N_\alpha \ll 1$; $N = 0.3$.

played good agreement between the results. For numbers M quite close to one, the function $\rho_{1,2}$ whose calculation can be realized by the approximation formula in [18]

$$\rho_{1,2} = \frac{1}{\sqrt{1-M^2}} \int_0^\infty [\Phi_1(x+t,\ 0) - \Phi_1(x-t,\ 0)] \frac{dt}{t},$$
$$\Phi_1(x,\ \xi) = \frac{M^2}{2\pi} \int_{-\infty}^{\infty} I(x,\ y,\ z) \exp(-i\xi y)\, dy \tag{12}$$

yields the main contribution to the density perturbation.

Comparison of the results of computations by means of (6)-(11) and by the approximate formula (12) performed for M = 0.95 yielded good agreement. The computations for numbers M > 0.95 were realized by means of (12).

The influence of the mesh domain dimensions on the accuracy of the computations was investigated. The results were compared for L_x, L_y = 6.4, 12.8, 25.6 including for different dimensions along the longitudinal (L_x) and transverse (L_y) coordinates to the flow as well as for magnified dimensions of the mesh domain used for the calculation of the field function u. It is established that it is sufficient to double the longitudinal dimension L_x and quadruple the transverse dimension L_y for the mesh domain of the function ρ_1 as compared with the mesh domain of the field u during calculation of the density function with error less than 1% in the M number range 0.8-0.95. As the transverse dimension L_y is doubled and the longitudinal dimension L_x is kept unchanged, the error in calculating the function ρ_1 is several percent while the error in calculating the field function u is less than a percent.

The method of expansion in discrete Fourier series with utilization of the fast Fourier transform permits filling in the gap for the subsonic mode in the set of linearized solutions of the propagation equation (1). Let us recall that this solution, which is valid in the geometric optics approximation ($L \ll ka^2$, $F \gg 1$) for weak self-action ($L \ll z_T$, $N \ll 1$) and for weak absorption ($L \ll \alpha^{-1}$, $N_\alpha \ll 1$) predicts defocusing of the Gaussian beam in isobaric approximation modes (heat conductive and convective) and passage from defocusing to focusing somewhere in the subsonic mode as the number M increases [5]. Application of the Fourier series expansion method permits this solution to be obtained in the following form convenient for computations

$$I = \exp\{-x^2 - y^2 - N_\alpha z - Nf(x,\ y)\},$$
$$f(x,\ y) = \frac{1}{2} \sum_m \sum_n \rho_{mn} \left[\left(\frac{\pi m}{L_x}\right)^2 + \left(\frac{\pi n}{L_y}\right)^2\right] \sin\alpha_m \sin\alpha_n + \tag{13}$$

$$+\sum_m\sum_n \rho_{mn}\frac{\pi m}{L_x}\cos\alpha_m\sin\alpha_n+\sum_m\sum_n \rho_{mn}\frac{\pi n}{L_y}\sin\alpha_m\sin\alpha_n \quad -2x\exp(-x^2-y^2)-(1-4y^2)\exp(-y^2)\int_{-\infty}^{x}\exp(-x'^2)dx',$$

$$\alpha_m=\frac{\pi m}{L_x}(x+L_x/2);\quad \alpha_n=\frac{\pi n}{L_y}(y+L_y/2).$$

Here ρ_{mn} are the spectral coefficients of the density perturbation functions $\rho_{1,2}$ that are related to the spectral coefficinets I_{mn} for the initial intensity distribution (for $z = 0$) by the relationships (11) while the thermal self-action parameter N equals the square of the dimensionless coordinate z: $N = z^2$.

Isochores and isophots are constructed in Fig. 3 for two values of the number M (M = 0.6 and 0.8) between which the diminution of the intensity peak at the selected distance $z_{phys} = 0.548z_T$ (N = 0.3) goes over into an increase as compared with the initial value. Just as the linearlized solutions for convective and supersonic modes [5], the linearized solution for the subsonic mode (13) yields a qualitatively correct results for sufficiently large values of the self-action parameter $N \leqslant 0.3$.

Summarizing, we note the following important situations. To construct the solution in the subsonic thermal self-action mode it is necesary to increase the computed field for the density function ρ_1 two-four times in the near-sonic domain $M > 0.8$ as compared with the computed domain for the field function u. For $M > 0.95$ the approximate solution of the Poisson equation can be used in which the dependence on the coordinate transverse to the gas flow is neglected. A sufficiently broad domain exists in the similarity parameter space (Mach number-Fresnel number-absorption parameter) in which the Gaussian beam is focused initially. Quasi-waveguide modes of Gaussian beam propagation are not detected. The linearized solution describes the main qualitative features of the thermal self-action effect in the subsonic gasdynamic mode, as in the convective and the supersonic modes which has been established earlier.

NOTATION

X, Y, Z, coordinates: u, complex electromagnetic field function: $F = ka^2/L$, Fresnel number; $k = 2\pi/\lambda$, wave number; λ, radiation wavelength; a, exponential beam radius, L, characteristic track length; $M = V_0/c$, Mach number; V_0, unperturbed gas flow velocity; c, sound speed therein; $N = \alpha L$, radiation absorption factor; $N = (L/z_T)^2$, nonlinearity (self-action) parameter; $z_T = a/\sqrt{\varepsilon(n_0 - 1)/n_0}$, length of thermal self-action; n_0, refractive index of the unperturbed gas; $\varepsilon = \alpha I_0 a/\rho_0 V_0 h_0$, scale of the gas density perturbation; I_0, characteristic radiation intensity; ρ_0, unperturbed gas density; h_0, unperturbed gas enthalpy; ρ_1, dimensionless gas density perturbation function; ρ_{mn}, I_{mn}, spectral coefficients for the gas density and the radiation intensity.

LITERATURE CITED

1. S. A. Akhmanov, A. P. Sukhorukov, and R. V. Khokhlov, Usp. Fiz. Nauk, 93, No. 1, 19-70 (1967).
2. G. A. Askar'yan, Usp. Fiz. Nauk, 111, No. 2, 250-260 (1973).
3. V. N. Lugovoi and A. M. Prokhorov, Usp. Fiz. Nauk, 111, No. 2, 203-247 (1973).
4. M. N. Kogan and A. N. Kucherov, Dokl. Akad. Nauk SSSR, 251, No. 3, 575-577 (1980).
5. M. N. Kogan and A. N. Kucherov, Izv. Vyssh. Uchebn. Zaved., Fizika, No. 2, 103-110 (1983).
6. D. C. Smith, Proc. IEEE, 65, No. 12, 1679-1714 (1977).
7. M. N. Kogan and A. N. Kucherov, Zh. Tekh. Fiz., 50, No. 3, 465-470 (1980).
8. V. A. Vysloukh, K. D. Egorov, and V. P. Kandidov, Vestn. Mosk. Univ., Ser. 3 Fiz. Astron., 21, No. 2, 16-20 (1980).
9. J. Wallace and J. Pasiak, Applied Optics, 15, No. 1, 218-222 (1976).
10. J. A. Fleck, J. R. Morris, and M. D. Feit, Applied Physics, 10, No. 2, 129-160 (1976).
11. K. D. Egorov, Vestn., Mosk. Univ., Ser. 3, Fiz. Astron., 20, No. 4, 105-106 (1979)
12. H. Harmuth, Journ. Math. Phys., 36, No. 3, 269-278 (1957).
13. L. G. Bradley and J. Herman, Journ. Opt. Soc. Amer., 61, No. 5, 668 (1971).
14. S. S. Chesnokov, K. D. Egorov, V. P. Kandidov, and V. A. Vysloukh, Intern. Journ. Numer. Methods in Engng., 14, No. 4, 1581-1591 (1979).
15. S. S. Chesnokov, Vestn. Mosk. Univ., Ser. 3, Fiz. Astron., 21, No. 6, 27-31 (1980).

16. Yu. N. Karamzin, Numerical Methods of Certain Nonlinear Optics Problems [in Russian], Preprint No. 73, Inst. Prikl. Matem. im M. V. Keldysh Akad. Nauk SSSR (1982).
17. A. N. Kucherov, Dokl. Akad. Nauk SSSR, 251, No. 2, 309-311 (1980).
18. V. V. Vorob'ev, Kvant. Élektron., 3, No. 3, 605-607 (1976).

COMPUTATION OF LAMINAR VISCOUS FLUID FLOWS IN ARBITRARY AXISYMMERIC CHANNELS

V. E. Karyakin, Yu. E. Karyakin, and A. Ya. Nesterov

UDC 532.516

A finite-difference method is proposed for computing flows in axisymmetric channels of arbitrary configuration in the presence of a swirling stream.

One of the widespread causes of fluid flows in modern power plant elements is axisymmetric motion. It is characteristic for diffuser and expander type channels, axiradial turbine channels, different kinds of branchpieces and is accompanied sufficiently often by a swirling stream that raises the intensity of the heat and mass transfer processes that occur.

Laminar fluid flow in the initial section of a straight annular channel is studied in the presence of a swirling stream in [1], while an annular channel with arbitrary generators is examined in [2]. The formation of stream separation zones near the channel walls has been established.

Swirling fluid flows in a straight cylindrical pipe without a central body have been examined in [3, 4]. A reversible flow domain with several recirculation centers occurs on the pipe axis for high values of the rotation parameter.

A computation of axiradial channels of arbitrary configuration in the presence of a swirling stream is performed in [5]. The influence of the Reynolds number and the rotation parameter on the fundamental stream characteristics has been investigated. An analogous problem is solved in [6] without taking swirling into account.

The stream function, vorticity, and the circumferential velocity are the main dependent variables in [1-6]. However, solution of the Navier–Stokes equations is realized more and more often with respect to the so-called physical variables (the velocity and pressure components). The mode of writing the Navier–Stokes equations that characterize fluid flow in arbitrary axisymmetric channels is set down below and a difference method is proposed for the solution of such problems.

As is known [8], the nonstationary motion of an incompressible viscous fluid in an arbitrary curvilinear nonorthogonal coordinate system x^1, x^2, x^3 is described by the following equations

$$\frac{\partial v_i}{\partial t}+\frac{\partial(\hat{v}^k\hat{v}_i)}{\partial x^k}=-\frac{\partial p}{\partial x^i}+\frac{1}{\mathrm{Re}}\frac{\partial}{\partial x^k}\left(\hat{g}^{kl}\frac{\partial\hat{v}_i}{\partial x^l}\right), \tag{1}$$

$$\frac{\partial\hat{v}^k}{\partial x^k}=0,\ i,\ k,\ l=1,\ 2,\ 3. \tag{2}$$

Here and henceforth, subscripts repeated twice assume summation over all their allowable values. The velocity vector components in the x^1, x^2, x^3 coordinate system are related to the Cartesian components by known tensory analysis relationships (α = 1, 2, 3):

$$v_i=u_\alpha\frac{\partial y_\alpha}{\partial x^i},\quad v^i=u_\alpha\frac{\partial x^i}{\partial y_\alpha},\quad u_\alpha=v_i\frac{\partial x^i}{\partial y_\alpha}=v^i\frac{\partial y_\alpha}{\partial x^i}, \tag{3}$$

while the quantities $\hat{v}_i$, $\hat{v}^i$, $\hat{g}^{k\ell}$ are determined by using matrices of the derivatives $\partial x^i/\partial y_\alpha$ and $\partial y_\alpha/\partial x^i$ fixed at the point of differentiation Q:

Leningrad Polytechnic Institute. Translated from Inzhenerno-Fizicheskii Zhurnal, Vol. 8, No. 1, pp. 42-49, January, 1990. Original article submitted September 19, 1988.

 0022-0841/90/5801-0034$12.50